

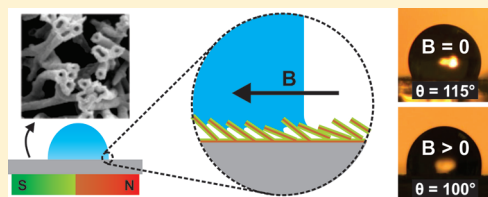
Magnetically Induced Decrease in Droplet Contact Angle on Nanostructured Surfaces

Qian Zhou,^{†,§} William D. Ristenpart,^{*,†,‡} and Pieter Stroeve[†]

[†]Department of Chemical Engineering & Materials Science and [‡]Department of Food Science & Technology, University of California Davis, Davis, California 95616, United States

[§]State Key Laboratory of Heavy Oil Processing, College of Science, China University of Petroleum, Beijing 102249

ABSTRACT: We report a magnetic technique for altering the apparent contact angle of aqueous droplets deposited on a nanostructured surface. Polymeric tubes with embedded superparamagnetic magnetite (Fe_3O_4) nanoparticles were prepared via layer-by-layer deposition in the 800 nm diameter pores of polycarbonate track-etched (PCTE) membranes. Etching away the original membrane yields a superparamagnetic film composed of mostly vertical tubes attached to a rigid substrate. We demonstrate that the apparent contact angle of pure water droplets deposited on the nanostructured film is highly sensitive to the ante situm strength of an applied magnetic field, decreasing linearly from $117 \pm 1.3^\circ$ at no applied field to $105 \pm 0.4^\circ$ at an applied field of approximately 500 G. Importantly, this decrease in contact angle did not require an inordinately strong magnetic field: a 15° decrease in contact angle was observed even with a standard alnico bar magnet. We interpret the observed contact angle behavior in terms of magnetically induced conformation changes in the film nanostructure, and we discuss the implications for reversibly switching substrates from hydrophilic to hydrophobic via externally tunable magnetic fields.



INTRODUCTION

Droplet contact angles depend sensitively on both surface energy and surface morphology, and accordingly many techniques have been developed to alter either the energetic or morphological characteristics of a surface to obtain desired wetting behavior.¹ For example, precise fabrication of nanoscale features on a surface allows surfaces to be superhydrophobic² or even superoleophobic³ by exploiting Cassie and/or Wenzel states;^{4–6} similarly, asymmetric nanofeatures guide spreading of droplets in preferred directions⁷ or in preferred shapes.⁸ Even without precise control of the nanoarchitecture, however, the surface energy and corresponding apparent contact angle can be modified by application of a sufficiently strong external field. The most well-known example involves applied electric fields, which give rise to the electrowetting effect⁹ that has found widespread application in optical lenses¹⁰ and lab-on-a-chip devices.¹¹ A key design constraint in electrowetting, however, is that there must be direct electrical contact between the substrate and droplet.⁹ In contrast, magnetic fields offer the possibility of nonintrusively modifying droplet contact angles, and indeed ferrofluids have been widely demonstrated to dramatically alter their contact angle and undergo a variety of instabilities in response to sufficiently strong magnetic fields.^{12,13} To date, however, magnetic modification of droplet contact angles has relied on the presence of ferromagnetic or superparamagnetic objects suspended within the liquid phase.

In this work, we report a magnetic technique for altering the apparent contact angle of pure water droplets devoid of any magnetically susceptible particles. The technique involves placement of water droplets onto a superparamagnetic film composed

of polymeric nanotubes infused with magnetite (Fe_3O_4) nanoparticles. We demonstrate that application of a sufficiently strong ante situm magnetic field (i.e., applied before the water droplet is placed onto the film) results in a markedly lower apparent contact angle, decreasing from $117 \pm 1.3^\circ$ at no applied field to $105 \pm 0.4^\circ$ at an applied field of approximately 500 G. In contrast, the post situm contact angle was insensitive to applied magnetic field strength. These results establish that the wetting behavior of water droplets unadulterated with magnetic particles may be manipulated with magnetic fields, opening the door to a wide range of possible applications in lab-on-a-chip devices or other applications where nonintrusive manipulation is desired.

FILM FABRICATION AND EXPERIMENTAL METHODOLOGY

Overview. To create a surface that alters its morphology in response to a magnetic field, two constraints must be satisfied: it must be superparamagnetic (so that reasonable magnetic fields induce a stable change), and it must be sufficiently nonrigid. To alter droplet contact angles, however, a third criterion must be satisfied: the characteristic length scale of the features on the surface must be sufficiently small so that the apparent roughness of the surface is modified by the magnetic field. Accordingly, to satisfy all three constraints, we sought to create flexible polymeric nanopillars with superparamagnetic properties. Polymeric nanopillars have been widely used to alter droplet contact angles,^{1,14} but simultaneous placement of superparamagnetic objects

Received: June 29, 2011

Revised: August 20, 2011

Published: August 31, 2011

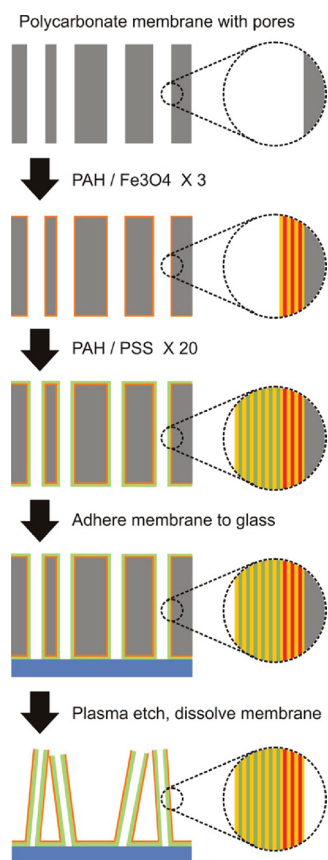


Figure 1. Schematic of the film fabrication procedure (not to scale).

within the nanopillars is not readily achievable using standard lithographic techniques.

Instead, we used a porous template method in combination with layer-by-layer (LbL) deposition. The LbL process for templates typically involves the sequential deposition of different species, such as polymers, nanoparticles, lipids, proteins, dyes, or other small molecules, into various porous templates, which are subsequently removed to yield free-standing nanotubes with tailored properties.¹⁵ Here we follow an LbL procedure similar to that used by Lee et al., who prepared freely suspended nanotubes with embedded magnetite nanoparticles.¹⁶ The key difference in this work is that we fabricated nanotubes still directly attached to a substrate, thus yielding a nanostructured superparamagnetic surface.

Preparation of the Fe₃O₄ Nanoparticles. Citrate-stabilized Fe₃O₄ nanoparticles were synthesized using the method reported by Sahoo et al.¹⁷ Briefly, a mixture containing 0.86 g of FeCl₂ and 1.40 g of FeCl₃ was prepared in 40 mL of deionized water (degassed by bubbling nitrogen prior to mixing) and heated to 80 °C under nitrogen. While vigorously stirring the mixture, 5 mL of NH₄OH was added by syringe and heated for an additional 30 min. The supernatant was decanted while the nanoparticles were retained in the reaction flask using a magnet, and then fresh water was added. Citric acid solution (2 mL, 0.5 g/mL) was added, and the reaction mixture was heated to 95 °C for 90 min. The reaction mixture was allowed to cool to room temperature under nitrogen. The nanoparticles were then rinsed with deionized water three times and dialyzed with DI water for 72 h. A transmission electron microscope (Phillips CM12 TEM) was used to image and size the synthesized Fe₃O₄ nanoparticles. The diameters of >200 particles were measured, resulting in a log-normal size distribution with an average diameter of 26 ± 9 nm.

Preparation of the Nanostructured Film. The film fabrication procedure is summarized in Figure 1. A polycarbonate tracked-etched

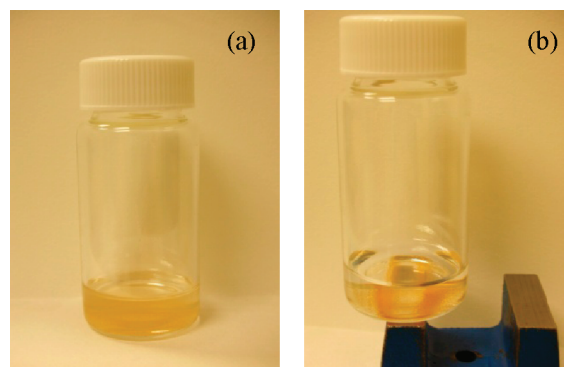


Figure 2. Behavior of (PAH/Fe₃O₄)₃(PAH/PSS)₂₀ tubes, freely suspended in alcohol solution, in response to a magnetic field. (a) No magnetic field. (b) Near an alnico magnet. Note the tubes (light brown color) concentrate at the regions of high magnetic field strength.

(PCTE) membrane with 800 nm diameter pores was used as the template. For the LbL deposition, we used polyallylamine hydrochloride (PAH) as the polycation and polystyrene sulfonate (PSS) as the polyanion; this combination has been widely used in LbL syntheses.¹⁸ Separate solutions of PAH and PSS were prepared at 10 mM (based on the repeat unit molecular weight) using DI water (>18 MΩ/cm), and the pH of both polyelectrolyte solutions and the rinsewater were all adjusted to 9.3. The LbL process consisted of alternating immersion of the membrane in PAH solution then Fe₃O₄ suspension a total of three times, followed by alternating immersion in PAH and PSS solutions a total of 20 times. Each immersion lasted 20 min, during which the polyelectrolytes or nanoparticles deposited on the exposed surfaces of the PCTE membrane. Between immersions, the membrane was rinsed by immersion in three successive beakers filled with pH-adjusted DI water, for 2, 2, and 1 min, respectively.

After all 46 LbL multilayers were deposited, the membrane was wetted with DI water and placed on an amine-treated glass substrate (which has positive residual surface charges) and then heated in an oven at 60 °C for 15 min to enhance adhesion between the membrane and the glass substrate. The membrane was then plasma etched (Harrick plasma cleaner PDC-32G) for 15 or more min, which selectively removed the multilayered film deposited on the exposed upper surface. Finally, the entire assembly was immersed in four separate beakers of fresh dichloromethane for 20, 2, 2, and 1 min, respectively, to dissolve the original PCTE membrane template.

Materials and Characterization. Poly(allylamine hydrochloride) (MW 56 000), poly(sodium 4-styrenesulfonate) (MW 70 000), FeCl₂, FeCl₃, citric acid monohydrate, silane-prep slides, and dichloromethane were purchased from Sigma-Aldrich and used as received. Polycarbonate track-etched membranes (10 μm thick, 47 mm total diameter, with 800 nm diameter pores) were purchased from GE Water & Process Technologies. The nanostructured films were imaged with a high-resolution scanning electron microscope (Philips XL30 SPEG SEM).

Contact Angle Measurements. Two different types of magnets were used to investigate the influence of magnetic field strength on the wetting behavior of droplets on the nanostructured films. First, an alnico bar magnet was used to qualitatively confirm that a “standard” or readily available magnetic field strength could induce a measurable change in apparent contact angle. Second, a round electromagnet (12 V DC, Magnatech Corp., model R-3030-12) was used to apply an adjustable magnetic field strength and obtain more systematic measurements. The substrate with nanostructured film was placed at the edge of the electromagnet, so that the magnetic field lines were mostly parallel to the surface. In both cases, within a few seconds following deposition (well after the droplet had reached a static configuration), the droplets

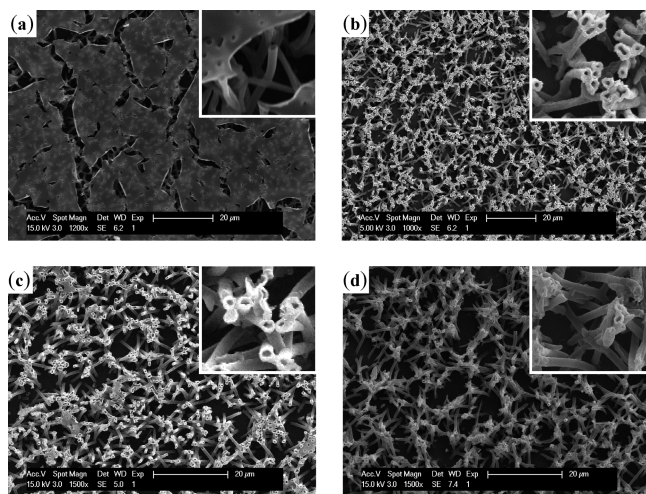


Figure 3. SEM images of the $(\text{PAH}/\text{Fe}_3\text{O}_4)_3(\text{PAH}/\text{PSS})_{20}$ films following plasma etching of various durations. (a) No etching; (b) 15 min; (c) 20 min; (d) 30 min. The scale bars are 20 μm ; the insets show a 10 \times magnification.

were imaged from the side using a high-resolution digital camera. The apparent contact angles^{19,20} were extracted from the images using standard image analysis techniques.

RESULTS AND DISCUSSION

To confirm that the nanotubes were superparamagnetic, we first prepared nanotubes without adhering them to a glass substrate, that is, skipping the third step in Figure 1. This procedure yielded a suspension of freely suspended nanotubes, in a fashion similar to that followed by Lee et al.¹⁶ Placing a magnet in close proximity to the suspension induced rapid migration of the tubes toward the magnet (Figure 2), confirming that the nanotubes were indeed superparamagnetic.

Including the surface adhesion step yielded films composed of mostly vertical nanotubes, the quality of which depended sensitively on the duration of the plasma etching step. Figure 3 shows representative films after dissolution of the original membrane but with different amounts of plasma etching. Without any plasma etching (Figure 3a), the surface is mostly flat with periodic holes (which represent the original locations of the track-etched pores) and with larger cracks where the film has broken apart. This flat film formed via LbL deposition on top of the original membrane, and following membrane dissolution remained connected to the majority of the nanotubes, reducing their mobility. Accordingly, the major purpose of the plasma etching step was to remove the flat film on top and to “free” the nanotubes. Representative films that resulted from 15, 20, and 30 min of plasma etching are shown respectively in Figure 3b–d. After 15 min of plasma etching, no evidence of the top film remains, and the majority of nanotubes tend to be curved and/or buckled, with most forming bundles in closer association; presumably, removal of the top film allowed dispersion forces to bring the tubes into closer proximity. Inspection of the tube cross sections indicates that the tube walls were approximately $0.3 \pm 0.02 \mu\text{m}$ thick; the Fe_3O_4 nanoparticles are not visible at this resolution and are presumably embedded within the polymer multilayers in the fashion observed by Lee et al.¹⁶ Longer periods of etching either had little observable effect, as is the case for 20 min of etching, or began to degrade the quality of

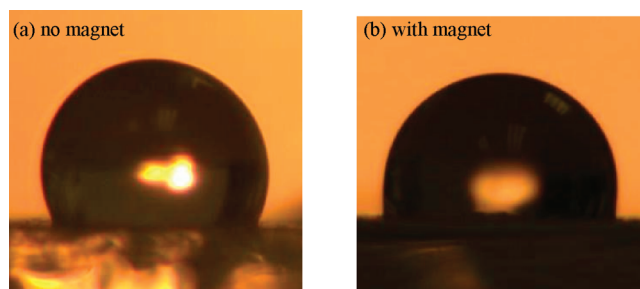


Figure 4. Representative images of 1 μL deionized water droplets placed on a nanostructured film similar to that shown in Figure 3b. In both cases, the droplet diameters are approximately 3 mm. (a) Without any magnetic field, the observed contact angle is 117°. (b) When the substrate is placed on top of a bar magnet, the observed contact angles are appreciably lower: 98° and 102° on the left- and right-hand sides of the droplet, respectively.

the tubes as seen in the partially “melted” look of the tubes evident in the film subjected to 30 min of etching. Accordingly, subsequent contact angle experiments were made on films with 15 min of plasma etching.

Placing water droplets on nanostructured films similar to the one shown in Figure 3B revealed a pronounced effect of applied magnetic field strength on the three-phase apparent contact angle. A water drop placed on a film in the absence of an applied magnetic field strength is shown in Figure 4a. The observed contact angle was $117 \pm 1.3^\circ$. Since the Young contact angle for PAH/PSS on unstructured (nominally flat) surfaces is approximately 55° ,²¹ it is clear that the nanotubes considerably increase the effective roughness of the substrate, an effect qualitatively consistent with previous observations of droplet contact angles on surfaces composed of nanopillars.¹ In contrast, when the same nanostructured film and glass substrate were placed on top of a bar magnet, the observed contact angle was significantly lower (Figure 4b). In this case, the observed contact angles were 98° and 102° on either side of the droplet, indicating that the magnetic field decreased the contact angle by approximately 15° . We emphasize that the only difference between the two experiments is that in the latter experiment the glass substrate was placed on top of a bar magnet prior to placement of the water droplet. Given that the measurements yielded standard deviations of 1–2°, it is clear that the decrease in contact angle is statistically significant.

To test reproducibility, we repeated the experiment several times on the same film and on different films (Figure 5). In each case, the apparent contact angle of water droplets placed on the film in the presence of the magnetic field was appreciably lower. The observed decrease in apparent contact angle was highly reproducible: after a droplet was allowed to dry, the apparent contact angle of subsequent drops placed on that film depended only on the presence or absence of the magnetic field, regardless of whether that film had previously had a droplet deposited and evaporated on it. Notably, the contact angle was only altered by the ante situm application of a magnetic field. The film had to be placed near the magnet before the water droplet was placed for the decrease in contact angle to be observed. If the water droplet was first deposited and then the substrate moved onto the magnet, no change in contact angle was observed.

Bar magnets are inconvenient for precisely modifying magnetic field strengths. To more precisely quantify the magnetic

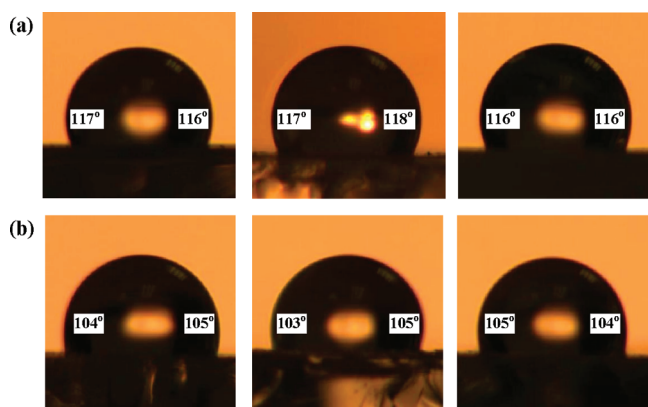


Figure 5. Representative images of 1 μL DI water droplets placed on the nanostructured surface to demonstrate reproducibility. (a) No magnetic field. (b) With magnetic field from a bar magnet.

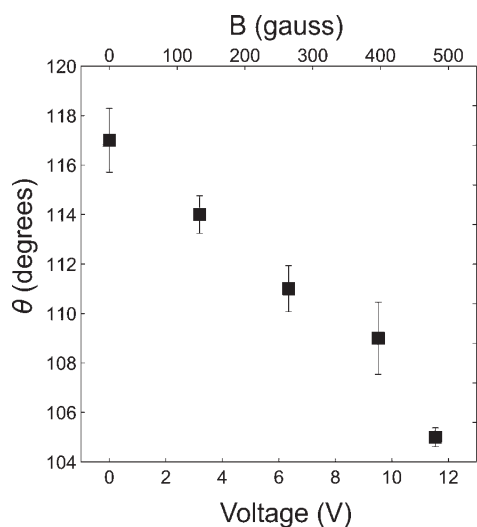


Figure 6. Apparent contact angle of 1 μL deionized water droplets placed on the nanostructured film as a function of the ante situm magnetic field strength. The bottom horizontal axis is the actual voltage applied to the electromagnet; the top horizontal axis is an estimate of the corresponding magnetic field strength. Error bars represent one standard deviation of three to five different droplets.

field dependence, we instead used a round electromagnet to systematically vary the magnetic field strength and measure the resulting apparent contact angle. The experimental trials were done in random order to reduce the possibility of systematic errors. The results indicate that the apparent contact angle decreases approximately linearly with the voltage applied to the electromagnet (Figure 6). Since the magnetic field strength for the iron-core electromagnet used here varies approximately linearly with current, the results in Figure 6 suggest that the contact angle likewise varies linearly with magnetic field strength, at least over the range of strengths applied here (0 to approximately 500 G).

Having demonstrated that applied magnetic fields alter the droplet contact angle, the next question is: how? Since the interfacial tension of the water itself is insensitive to the magnetic field, it is clear that the magnetic field must instead interact with the superparamagnetic nanoparticles embedded in the

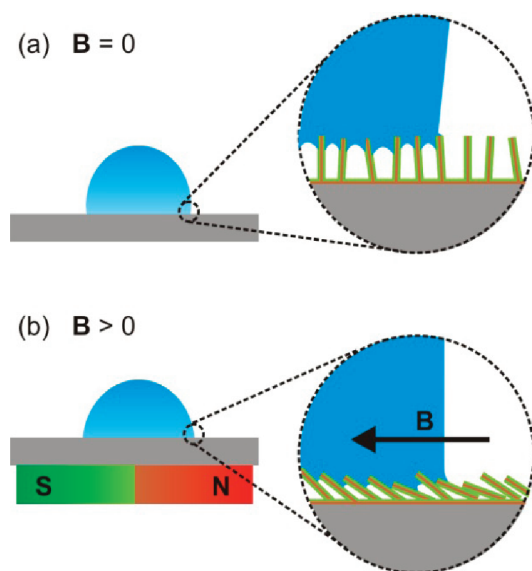


Figure 7. Schematic illustration of the water droplet on the surface of the nanostructured film under different magnetic field intensities.

nanotubes to somehow alter the properties of the film. The chemical properties of the nanotubes do not change magnetically, so the simplest explanation is that the magnetic field alters the conformation of the nanotubes, changing the effective roughness of the surface. This proposed mechanism is sketched qualitatively in Figure 7. Initially, most of the nanotubes are approximately vertical, consistent with the SEM image in Figure 3b. Because there are sizable separations between the nanotubes, the droplet can rest on top of the pillars with air trapped below (i.e., a Cassie state). In contrast, when the magnetic field is applied, the nanotubes experience a torque in the direction of the applied field.²² This torque causes the nanotubes to bend in the direction of the field. Because the outer layer of PAH on the nanotubes is hydrophilic, this conformation change increases the amount of hydrophilic surface accessible to the water droplet, increasing the wettability of the surface. It is unclear whether the wetting state in the presence of the magnetic field is a modified Cassie state, a Wenzel state, or a more complicated “mixed” wetting state;^{23–26} additional experiments are needed to elaborate the wetting state in the presence of the magnetic field.

Regardless of the wetting state, the lack of a response to a post situm magnetic field can be considered in terms of energetic arguments. When the nanotubes are surrounded only by air, the main resistance to magnetically induced motion is the bending modulus of the nanotubes themselves. When the magnetic field is removed, the nanotubes return to their preferred orientation; this interpretation is consistent with the observed lack of dependence on the history of the applied magnetic field. In contrast, when a drop is already deposited on top of the nanotubes, additional energy must be expended to overcome the capillary forces at the solid/air/water interfaces on each nanotube in order for the tubes to bend. Presumably, our electromagnet did not provide sufficient magnetic field strength to overcome the capillary forces, and consequently, the post situm contact angle was unchanged. Nonetheless, the results suggest that stronger magnetic fields, or liquids with lower capillary energies, might allow the post situm contact angle to be altered dynamically.

CONCLUSIONS

In summary, we demonstrate a method to magnetically reduce the contact angle of pure water droplets using superparamagnetic nanostructured substrates. The contact angle of the droplets decreased approximately linearly with the ante situm value of the applied magnetic field strength, a result we interpret in terms of magnetically induced conformation changes in the nanotubes on the substrate. This interpretation suggests that even larger changes in apparent contact angle could be obtained by increasing the flexibility of the nanotubes and optimizing the spacing between them, so that a transition between Cassie and Wenzel states could be induced by the absence or presence of the applied magnetic field. In our observations, the contact angle did not vary with the post situm value of the magnetic field strength, at least over the range of strengths tested. In this sense, the behavior observed here with water droplets is fundamentally different from standard electrowetting or magnetowetting of ferrofluids, which alter contact angle dynamically in response to changing field strengths. Nonetheless, the results presented here point the way toward a possible nonintrusive method for dynamically controlling the apparent contact angle of water drops using applied magnetic fields.

AUTHOR INFORMATION

Corresponding Author

*E-mail: wdristenpart@ucdavis.edu.

ACKNOWLEDGMENT

Support for Q.Z. was provided by the State Scholarship Fund of the China Scholarship Council and the National Natural Science Foundation of China (No. 50702077). We thank Dr. Dat Quach for helping with the TEM measurements.

REFERENCES

- (1) Quere, D. Wetting and roughness. *Ann. Rev. Mater. Res.* **2008**, *38*, 71–99.
- (2) Lau, K. K. S.; Bico, J.; Teo, K. B. K.; Chhowalla, M.; Amaratunga, G. A. J.; Milne, W. I.; McKinley, G. H.; Gleason, K. K. Superhydrophobic carbon nanotube forests. *Nano Lett.* **2003**, *3*, 1701–1705.
- (3) Tuteja, A.; Choi, W.; Ma, M. L.; Mabry, J. M.; Mazzella, S. A.; Rutledge, G. C.; McKinley, G. H.; Cohen, R. E. Designing superoleophobic surfaces. *Science* **2007**, *318*, 1618–1622.
- (4) McHale, G. Cassie and Wenzel: Were they really so wrong? *Langmuir* **2007**, *23*, 8200–8205.
- (5) Li, X. M.; Reinhoudt, D.; Crego-Calama, M. What do we need for a superhydrophobic surface? A review on the recent progress in the preparation of superhydrophobic surfaces. *Chem. Soc. Rev.* **2007**, *36*, 1350–1368.
- (6) Koishi, T.; Yasuoka, K.; Fujikawa, S.; Ebisuzaki, T.; Zeng, X. C. Coexistence and transition between Cassie and Wenzel state on pillared hydrophobic surface. *Proc. Natl. Acad. Sci. U.S.A.* **2009**, *106*, 8435–8440.
- (7) Chu, K. H.; Xiao, R.; Wang, E. N. Uni-directional liquid spreading on asymmetric nanostructured surfaces. *Nat. Mater.* **2010**, *9*, 413–417.
- (8) Courbin, L.; Denieul, E.; Dressaire, E.; Roper, M.; Ajdari, A.; Stone, H. A. Imbibition by polygonal spreading on microdecorated surfaces. *Nat. Mater.* **2007**, *6*, 661–664.
- (9) Mugele, F.; Baret, J. C. Electrowetting: From basics to applications. *J. Phys.: Condens. Matter* **2005**, *17*, R705–R774.
- (10) Berge, B.; Peseux, J. Variable focal lens controlled by an external voltage: An application of electrowetting. *Eur. Phys. J. E* **2000**, *3*, 159–163.
- (11) Pollack, M. G.; Fair, R. B.; Shenderov, A. D. Electrowetting-based actuation of liquid droplets for microfluidic applications. *Appl. Phys. Lett.* **2000**, *77*, 1725–1726.

- (12) Chen, C. Y.; Cheng, Z. Y. An experimental study on Rosensweig instability of a ferrofluid droplet. *Phys. Fluids* **2008**, *20*, 5.
- (13) Nguyen, N. T.; Zhu, G. P.; Chua, Y. C.; Phan, V. N.; Tan, S. H. Magnetowetting and Sliding Motion of a Sessile Ferrofluid Droplet in the Presence of a Permanent Magnet. *Langmuir* **2010**, *26*, 12553–12559.
- (14) Quere, D.; Reyssat, M. Non-adhesive lotus and other hydrophobic materials. *Philos. Trans. R. Soc., A* **2008**, *366*, 1539–1556.
- (15) Wang, Y.; Angelatos, A. S.; Caruso, F. Template synthesis of nanostructured materials via layer-by-layer assembly. *Chem. Mater.* **2008**, *20*, 848–858.
- (16) Lee, D.; Cohen, R. E.; Rubner, M. F. Heterostructured magnetic nanotubes. *Langmuir* **2007**, *23*, 123–129.
- (17) Sahoo, Y.; Goodarzi, A.; Swihart, M. T.; Ohulchanskyy, T. Y.; Kaur, N.; Furlani, E. P.; Prasad, P. N. Aqueous ferrofluid of magnetite nanoparticles: Fluorescence labeling and magnetophoretic control. *J. Phys. Chem. B* **2005**, *109*, 3879–3885.
- (18) Arys, X.; Jonas, A. M.; Laschewsky, A.; Legras, R.; Mallwitz, F. In *Supramolecular Polymers*; Ciferri, A., Ed.; Taylor & Francis: Boca Raton, FL, 2005; Vol. 2, pp 651–710.
- (19) de Gennes, P. G.; Brochard-Wyart, F.; Quere, D. *Capillarity and Wetting Phenomena*; Springer: New York, 2004.
- (20) Marmur, A. Soft contact: measurement and interpretation of contact angles. *Soft Matter* **2006**, *2*, 12–17.
- (21) Yoo, D.; Shiratori, S. S.; Rubner, M. F. Controlling bilayer composition and surface wettability of sequentially adsorbed multilayers of weak polyelectrolytes. *Macromolecules* **1998**, *31*, 4309–4318.
- (22) Jackson, J. D. *Classical Electrodynamics*, 2nd ed.; John Wiley & Sons: New York, 1975.
- (23) Bico, J.; Thiele, U.; Quere, D. Wetting of textured surfaces. *Colloids Surf., A* **2002**, *206*, 41–46.
- (24) Miwa, M.; Nakajima, A.; Fujishima, A.; Hashimoto, K.; Watanabe, T. Effects of the surface roughness on sliding angles of water droplets on superhydrophobic surfaces. *Langmuir* **2000**, *16*, 5754–5760.
- (25) Bormashenko, E. Wetting transitions on biomimetic surfaces. *Philos. Trans. R. Soc., A* **2010**, *368*, 4695–4711.
- (26) Bormashenko, E. General equation describing wetting of rough surfaces. *J. Colloid Interface Sci.* **2011**, *360*, 317–319.